The MoT-ICE: a new high-resolution wave-propagation algorithm based on Fey's Method of Transport [1]

Sebastian Noelle
Institut für Angewandte Mathematik
Universität Bonn
Wegelerstr. 10
53115 Bonn, Germany
noelle@iam.uni-bonn.de

ABSTRACT *The numerical solution of multi-dimensional systems of conservation laws is dominated by upwind-schemes based on one-dimensional Riemann-solvers. Such schemes neglect the physical directions of wave-propagation and replace them by the grid-directions. One of the algorithmic alternatives is Fey's Method of Transport (MoT). Similarly to its one-dimensional fore-runner, the Steger-Warming-Scheme, the MoT suffers from an inconsistency at sonic points. Here we derive a new version of Fey's multi-dimensional flux-vector-splitting and a globally consistent second-order-accurate characteristic scheme based on Interface-Centered-Evolution, the MoT-ICE. Numerical experiments show the stability, accuracy and efficiency of the new scheme.*

Key Words: Systems of Conservation Laws, Multi-dimensional Flux-Vector-Splitting, Fey's Method of Tranport.

1. Introduction

Since the work of Godunov, Van Leer, Harten-Lax and Roe, the numerical solution of systems of hyperbolic conservation laws is dominated by Riemann-solver based schemes (see [HIR 90] for the classical references). These one-dimensional schemes are extended to several space-dimensions either by using dimensional-splitting on cartesian grids or by the finite-volume approach on un-

[1] Invited plenary lecture. To appear in: "Proceedings of the Second International Symposium on Finite Volumes for Complex Applications – Problems and Perspectives", Duisburg, Germany, July 1999. Supported by DFG-SPP ANumE.

structured grids. For both approaches, convergence and error estimates have been established for multi-dimensional **scalar** conservation laws, see for example the results and references in [CCL 94, KNR 95, NOE 96, WN 99]. Naturally, there are no comparable results for multi-dimensional **systems**, since no existence and uniqueness of the p.d.e.'s is known in this case.

The first systematic criticism of using one-dimensional Riemann-solvers for multi-dimensional gas-dynamics goes back to Roe himself [ROE 86]: the Riemann-solver is applied in the grid- rather than the flow-direction, which may lead to a misinterpretation of the local wave-structure of the solution. A description of a number of failings of exact and approximate Riemann-solvers for the two-dimensional Euler-equations of gasdynamics may be found in Quirk's paper [QUI 94]. LeVeque and Walder [LW 92] present difficulties of Godunov's scheme for strong two-dimensional shockwaves arising in astrophysical flows and propose the use of rotated Riemann-solvers. In [ROE 91, NOE 94] Roe and Noelle study oscillations generated by dimensional-splitting-schemes for a prototype linear system.

Since the mid-eighties, Roe, Deconinck, Van Leer and many others developed the so-called fluctuation-splitting schemes for the equations of gasdynamics. In these schemes the divergence of the multi-dimensional flux-vector (called fluctuation) is split according to a grid-independent wave model (see [VNL 92] for references). In [NOE 94], the author developed a fluctuation-splitting-scheme for a 2x2 model problem which cures the directional effects exhibited by dimensional-splitting-schemes. However, this fluctuation-splitting-scheme seems to be very dissipative for non-stationary problems.

Another multi-dimensional approach is the Corner-Transport-Upwind (CTU) scheme of Colella [COL 90]. Here waves are not only propagated to the neighbors which join a common side with a cell, but also to the corner cells. LeVeque's wave-propagation-algorithm, which forms the backbone of the publicly available software-package CLAWPACK, splits one-dimensional fluxes in the transverse directions and propagates them to the corner cells (see [LEV 97] and the references therein). In [BT 97], Billet and Toro introduce weighted-average-flux (WAF) schemes with good multi-dimensional upwinding- and stability-properties.

In this paper we follow the flux-vector-splitting approach, which was first proposed by Steger and Warming [SW 81] in one space-dimension. Instead of decomposing the divergence of the flux-vector, as in the fluctuation-splitting schemes of Roe et.al., the conservative variables and the flux-vector themselves are split (see [HIR 90], Ch.20.2). In his dissertation, Fey developed a multi-dimensional version of the Steger-Warming-scheme, and called it Method of Transport (MoT). This scheme integrates the acoustic waves over the entire Mach-cone (see also [LMW 97] for recent related progress). Subsequently Fey, Jeltsch et.al. simplified the MoT and expanded it in various directions (for references, see [FJMM 97, FEY 98a, FEY 98b]).

The starting point of this work are the papers [FEY 98b, FJMM 97]. In these papers, the MoT takes the following form: Step 1. A multi-dimensional wave-model leads to a reformulation of the conservation law as a set of nonlinearly coupled advection equations. Step 2. At the beginning of each timestep, the system is linearized and decomposed into a set of scalar advection equations with variable coefficients. Step 3. The solution of each scalar advection equation at the end of the timestep is computed using a characteristic scheme. Step 4. The solution is projected back onto the conservative variables using the wave-model of Step 1.

Our own contribution to Fey's method may be summarized as follows: Given a multi-dimensional wave-model, we simplify Step 2 by distinguishing clearly between linearization and decomposition error. This makes it possible to write down a general second-order-correction term for the decomposition error in a single line. Then we discuss the first-order version of Fey's characteristic scheme (Step 3) and show an inconsistency of the numerical scheme on the scalar level. Subsequently, we derive new first- and second-order characteristic schemes which are globally consistent. Due to the simpler second-order-correction term for the decomposition error and a particularly simple choice of numerical transport-velocities our second-order scheme needs only 2.2 times the CPU-time of the first order scheme, and is very efficient.

Fey's transport algorithm might be called MoT-CCE, since his scalar scheme uses Cell-Centered-Evolution. We call our new scheme, which is based on Interface-Centered-Evolution, MoT-ICE.

In Section 2, we discuss the multi-dimensional wave-models and the linearization and decomposition steps. In Section 3, we show the inconsistency of the MoT-CCE and present the MoT-ICE. In Section 4, we give numerical experiments. Finally, in Section 5, we discuss topics for future research.

This is a report on work in progress. The proofs of the theoretical results in Sections 2 and 3 as well as several important implementation details in Section 4 will be given in the forthcoming paper [NOE 99].

The author would like to thank Dr. Michael Fey and Christian von Törne for stimulating discussions on the Method of Transport. This work was supported by DFG-SPP ANumE. The hospitality of Dr. Fey, Prof. Jeltsch and his group during a visit at ETH Zürich is gratefully acknowledged.

2. Decomposition of multi-dimensional hyperbolic systems into scalar advection equations

In this section, we recall Fey's advection form and give a general second-order-accurate linearisation and decomposition of systems which can be written in advection form.

2.1. *A general framework for multi-dimensional flux-vector-splitting*

Consider a multi-dimensional system of n conservation laws in d space dimensions,

$$\partial_t U + \nabla \cdot \mathbf{f}(U) = 0 \tag{1}$$

where $U : \mathbf{R}^d \times \mathbf{R}_+ \to \mathbf{R}^n$ is the state-vector and $\mathbf{f} : \mathbf{R}^n \to \mathbf{R}^{n \times d}$ the flux-vector. The following framework for multi-dimensional flux-vector-splitting (FVS) has been developed by Fey, Jeltsch and collaborators [FJMM 97]:

Definition 1 *A* ***wave-model*** *for (1) is a set of $L \geq 1$ mappings*

$$\begin{aligned} S_l &: \mathbf{R}^n \to \mathbf{R}^n, \qquad l = 1 \dots L \\ \mathbf{a}_l &: \mathbf{R}^n \to \mathbf{R}^d, \qquad l = 1 \dots L \end{aligned}$$

which satisfy the consistency conditions

$$\sum_{l=1}^{L} S_l = Id \tag{2}$$

and

$$\sum_{l=1}^{L} S_l \; \mathbf{a}_l^T = \mathbf{f}. \tag{3}$$

Given a wave-model, the conservation law (1) may be rewritten in the following **advection form**:

$$\sum_{l=1}^{L} \left(\partial_t \; S_l(U) + \nabla \cdot (S_l(U) \; \mathbf{a}_l(U)^T) \right) = 0. \tag{4}$$

Wave-models for the wave-equation, the equations of isentropic and non-isentropic gas dynamics and the equations of ideal magneto-hydrodynamics may be found in [FJMM 97]. Common to all of them is a finite set of acoustic waves which approximate the Mach-cone (typically four waves in two space-dimensions). For the Euler-equations one adds an entropy-wave, and for the MHD-equations, the two Alfvén and possibly some slow magneto-acoustic waves.

2.2. *Decomposition into scalar advection equations*

Let us see how the advection form can be used when advancing the solution for a single timestep $k = \Delta t$. Ideally, one would like to set each summand in (4) to zero seperately. As we shall see below, this will lead to an error of $\mathcal{O}(k^2)$ during each time-step, limiting the overall accuracy of the scheme to first-order.

The following linearisation will be helpful in order to obtain a second-order-accurate decomposition:

Lemma 2 *(linearisation) Let U be a smooth solution of (1), $k = \Delta t > 0$. Let*

$$\begin{array}{rccc} V: & \mathbf{R}^d \times [t_n, t_n + k] & \rightarrow & \mathbf{R}^n \\ \widetilde{\mathbf{a}}_l: & \mathbf{R}^d & \rightarrow & \mathbf{R}^d \end{array}$$

satisfy

$$\widetilde{\mathbf{a}}_l = \mathbf{a}_l(U(t_n)) + \frac{k}{2}\,\partial_t\,\mathbf{a}_l(U(t_n)) + \mathcal{O}(k^2)$$

and

$$\begin{array}{c} \partial_t\,V + \nabla \cdot \sum_{l=1}^{L} S_l(V)\,\widetilde{\mathbf{a}}_l^T = 0 \\ V(t_n) = U(t_n). \end{array} \tag{5}$$

Then

$$V(t_n + k) - U(t_n + k) = \mathcal{O}(k^3).$$

The proofs of this and the following results will appear in [NOE 99]. Note that the approximate transport velocities $\widetilde{\mathbf{a}}_l$ are now *prescribed* coefficients which depend on space but not on time. System (5) is still *nonlinear* in V. It is, however, *linear* in the components $S_l(V)$, since $V = \sum_{l=1}^{L} S_l(V)$.

Next let us decompose the linearized advection form (5) by setting each summand to zero seperately: Let

$$W := \sum_{l=1}^{L} W_l : \mathbf{R}^d \times [t_n, t_n + k] \rightarrow \mathbf{R}^n$$

satisfy

$$\begin{array}{c} \partial_t\,W_l + \nabla \cdot (W_l\,\widetilde{\mathbf{a}}_l^T) = 0 \\ W_l(t_n) = S_l(U(t_n)). \end{array}$$

Then

$$W(t_n + k) - V(t_n + k) = \frac{k^2}{2}\,\nabla \cdot \left(\sum_{l=1}^{L} T_l\,\mathbf{a}_l^T\right) +\ \mathcal{O}(k^3)$$

where $T_l = T_l(U(t_n), \nabla \cdot U(t_n))$ is given by

$$T_l := \nabla \cdot \left(S_l(U(t_n))\,\mathbf{a}_l(U(t_n))^T\right) - S_l'(U(t_n))\ \ \nabla \cdot \mathbf{f}(U(t_n)).$$

Therefore, this naive ansatz leads to a first-order decomposition error. Taking a closer look at the leading part of the error, we note that

$$\sum_{l=1}^{L} T_l = \sum_{l=1}^{L} \left(\nabla \cdot \left(S_l\,\mathbf{a}_l^T\right) - S_l'\ \nabla \cdot f\right) = \left(I - \left(\sum_{l=1}^{L} S_l\right)'\right) \nabla \cdot f = 0,$$

since

$$\left(\sum_{l=1}^{L} S_l\right)' = (Id)' = I.$$

This can be used in order to derive a second-order-accurate decomposition of (5) respectively (4).

Theorem 3 *(second-order-accurate decomposition) Let*

$$Z := \sum_{l=1}^{L} Z_l : \ \mathbf{R}^d \times [t_n, t_n + k] \to \mathbf{R}^n$$

satisfy

$$\partial_t \ Z_l + \nabla \cdot (Z_l \ \widetilde{\mathbf{a}}_l^T) = 0$$
$$Z_l(t_n) = S_l(U(t_n)) + \tfrac{k}{2} \ T_l(U(t_n), \nabla \cdot U(t_n)).$$

Then

$$Z(t_n + k) - U(t_n + k) = \mathcal{O}(k^3).$$

For the Euler equations and the shallow-water equations, Morel, Fey and Maurer have also derived a second-order-accurate decomposition into linear advection equations. Instead of evaluating the velocities at the half-timestep, as done in Lemma 2, they freeze them at the original timestep. As a consequence, the linearization- and decomposition-errors are not seperated, and the second-order-correction terms become more involved.

3. Solving the scalar advection equations by characteristic schemes

The linearisation and decomposition given in the previous section leads us, at the beginning of each timestep, to a set of scalar transport equations of the form

$$\partial_t \ \varphi + \nabla \cdot (\varphi \ \mathbf{a}^T) = 0. \tag{6}$$

For the rest of this section, we consider the velocity-vector $\mathbf{a} : \mathbf{R}^d \times \mathbf{R}_+ \to \mathbf{R}^d$ to be a given function of $\mathbf{x}$ and t. The function $\varphi : \mathbf{R}^d \times \mathbf{R}_+ \to \mathbf{R}$ is the unknown, and initial data are prescribed at $t = t_n := nk$,

$$\varphi(x, t_n) = \varphi_D(x).$$

These equations may be solved by introducing characteristics $\mathbf{z}(\tau; \mathbf{x}, t)$ by

$$\begin{aligned} \mathbf{z} : \mathbf{R}_+ \times \mathbf{R}^d \times \mathbf{R}_+ &\to \mathbf{R}^d \\ \mathbf{z}(t; \mathbf{x}, t) &= \mathbf{x} \\ \partial_\tau \mathbf{z}(\tau; \mathbf{x}, t) &= \mathbf{a}(\mathbf{z}, \tau). \end{aligned}$$

Since the flux-vector $\varphi \mathbf{a}^T$ is always parallel to the characteristics, we have the following

Figure 1: Backwards characteristic transport of cell K_{ij}. The region bounded by the curved lines is $\mathbf{z}(t_n; K_{ij}, t_{n+1})$, and the dashed lines are backwards characteristic curves issuing from the corners of cell K_{ij} at time t_{n+1}.

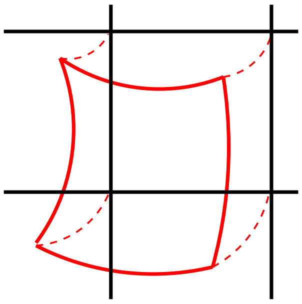

Lemma 4 *For all $K \subset \mathbf{R}^d$, $t, \tau \in \mathbf{R}_+$*

$$\frac{d}{d\tau} \int\limits_{\mathbf{z}(\tau;K,t)} \varphi(\mathbf{x}, \tau)\, d\mathbf{x} = 0.$$

3.1 *Characteristic schemes*

We would like to use Lemma 4 to construct numerical methods for solving (6). For simplicity, we restrict the analysis from now on to two space-dimensions, and use the notation $\mathbf{x} = (x, y) \in \mathbf{R}^2$ for the space variable and $\mathbf{a} = (a, b) \in \mathbf{R}^2$ for the velocity field.

Let $K_{ij} \subset \mathbf{R}^2$ be the cells of a uniform cartesian grid with mesh-size $h = \Delta x = \Delta y$, and recall that $k = \Delta t$ is the timestep. Due to Lemma 4,

$$\int\limits_{K_{ij}} \varphi(\mathbf{x}, t_{n+1})\, d\mathbf{x} = \sum_{i',j'} \left(\int\limits_{K_{i'j'} \cap \mathbf{z}(t_n; K_{ij}, t_{n+1})} \varphi_D(\mathbf{x})\, d\mathbf{x} \right).$$

Note that $K_{i'j'} \cap \mathbf{z}(t_n; K_{ij}, t_{n+1})$ is that part of $K_{i'j'}$ that will be mapped to K_{ij} by the characteristic flow from time t_n to time t_{n+1} (compare Figure 1).

Definition 5 *A **characteristic scheme** for (6) is given by*

$$\begin{aligned} \overline{\varphi}_{ij}^{0} &:= \tfrac{1}{|K_{ij}|} \textstyle\int_{K_{ij}} \varphi(\mathbf{x}, 0)\, d\mathbf{x} \\ \overline{\varphi}_{ij}^{n+1} &:= \sum_{i',j'} \overline{\varphi}_{i'j'}^{ij} := \sum_{i',j'} \tfrac{1}{|K_{ij}|} \textstyle\int_{K_{i'j'}^{ij}} \varphi_R(\mathbf{x})\, d\mathbf{x}, \end{aligned}$$

where φ_R is a piecewise smooth spatial reconstruction of $\varphi(\cdot, t_n)$, and $K_{i'j'}^{ij}$ an approximation of $K_{i'j'} \cap \mathbf{z}(t_n; K_{ij}, t_{n+1})$.

For the piecewise smooth spatial reconstruction of $\varphi(\cdot, t_n)$ we will either use piecewise constant or piecewise linear functions. We will label the corresponding schemes **P0** resp. **P1**. For the moment, let us consider schemes using piecewise constant reconstructions and focus on the approximation of the characteristic flow.

3.2 *Cell-Centered-Evolution: the MoT-CCE*

In a series of papers (see [FEY 98b, FJMM 97] and the references therein), Fey and collaborators have used the following approximation of the characteristic flow, which we will call **C**ell-**C**entered-**E**volution:

In each cell $K_{i'j'}$, consider the local characteristic flow defined by

$$\begin{aligned} \mathbf{z}_{ij}^n(t; \mathbf{x}, t) &= \mathbf{x} \\ \partial_\tau \mathbf{z}_{ij}^n(\tau; \mathbf{x}, t) &\equiv \mathbf{a}(x_i, y_j, t_n). \end{aligned}$$

Then set

$$K_{i'j'}^{ij} := K_{i'j'} \cap \mathbf{z}_{ij}^n(t_n; K_{ij}, t_{n+1}).$$

In one space-dimension this leads to the following algorithm:

$$\begin{aligned} \overline{\varphi}_i^{n+1} &:= \overline{\varphi}_{i-1}^i + \overline{\varphi}_i^i + \overline{\varphi}_{i+1}^i \\ &= \lambda\,(a_{i-1})_+\,\overline{\varphi}_{i-1} + (1 - \lambda|a_i|)\,\overline{\varphi}_i \\ &\quad -\lambda\,(a_{i+1})_-\,\overline{\varphi}_{i+1} \end{aligned} \tag{7}$$

where $\lambda := k/h$ and the subscripts $\pm$ denote the positive resp. negative part of a quantity. Fey calls his scheme **MoT** ("Method of Transport"), and therefore we will use the acronym **MoT-CCE-P0**.

Let us discuss the consistency of the MoT-CCE-P0 with the differential equation (6). If $\mathbf{a}$ is constant, then (7) coincides with the first-order upwind scheme. For variable coefficients the situation is more complex:

Example 6 *Let us consider the case*

$$a(x, t) = -x$$

corresponding to a compressive wave ($\nabla \cdot \mathbf{a} < 0$). For constant initial data,

$$\varphi_D(x) \equiv 1,$$

the exact solution remains constant in space but grows exponentially in time,

$$\varphi(x, t) \equiv e^t.$$

The approximate solution produced by the MoT-CCE-P0 is

$$\overline{\varphi}_i^n = \begin{cases} (1+k)^n & i \neq 0 \\ 2\,(1+k)^n - 1 & i = 0\,. \end{cases}$$

As k tends to zero with λ fixed, this solution converges to

$$\varphi^{\text{approx}}(x,t) := \begin{cases} e^t & x \neq 0 \\ 2\,e^t - 1 & x = 0\,. \end{cases}$$

Thus (7) is inconsistent with the differential equation (6) at the "sonic" point $x = 0$, where the transport velocity a changes sign. The cell-centered-evolution leads to an inconsistent approximation of $\nabla \cdot \mathbf{a}$, which takes the value 2 instead of 1. An analogous inconsistency occurs for the case of an expansive wave, $\nabla \cdot \mathbf{a} > 0$. We omit the details.

This difficulty was already described by Steger and Warming [SW 81] in 1981: the numerical flux produced by their splitting is not continuously differentiable at sonic points for the equations of gas-dynamics. This results in so-called "glitches" at sonic points. Subsequently, Van Leer developed a splitting with continuously differentiable fluxes (compare [HIR 90], Ch. 20.2.3).

In her dissertation, Morel [MOR 97] also observed glitches at sonic points for two-dimensional shallow-water-computations carried out with the MoT-CCE-P0, and generalized the Van-Leer-flux-vector-splitting to two space-dimensions in order to remove these numerical artefacts. However, this slows down the algorithm considerably, and Morel herself remarks that her method does not seem to be generalizable to second-order-accuracy.

Finally, let us remark that in Example 6 above, the MoT-CCE-P0 diverges in the L^∞-norm, but converges in L^1. Moreover, this inconsistency does not occur when one approximates the velocity field a by piecewise linear functions.

3.3 *Interface-Centered-Evolution: the MoT-ICE*

In the following we will derive a consistent alternative to the cell-centered-evolution discussed above. Since the new scheme will approximate the transport velocities at the interfaces between the cells, we will call it **MoT-ICE** for **I**nterface-**C**entered-**E**volution.

Instead of using a cell-centered approximation of the local characteristic flow to decompose K_{ij}, we now define auxiliary transport velocities $\widehat{a}^n_{i+\frac{1}{2},j}$ on the vertical interfaces

$$I_{i+\frac{1}{2},j} := \{x_{i+\frac{1}{2}}\} \times [y_{j-\frac{1}{2}}, y_{j+\frac{1}{2}}]$$

resp. $\widehat{b}^n_{i,j+\frac{1}{2}}$ on the horizontal interfaces

$$J_{i,j+\frac{1}{2}} := [x_{i-\frac{1}{2}}, x_{i+\frac{1}{2}}] \times \{y_{j+\frac{1}{2}}\}$$

between the cells. Let $\lambda = k/h$ be fixed and suppose that the CFL-condition

$$\lambda \max_{i,j}(|\widehat{a}^n_{i+\frac{1}{2},j}|, |\widehat{b}^n_{i,j+\frac{1}{2}}|) \leq 1 \tag{8}$$

Figure 2: Auxiliary transport velocities and approximate characteristic decomposition of a two-dimensional cell K_{ij} via Interface-Centered-Evolution.

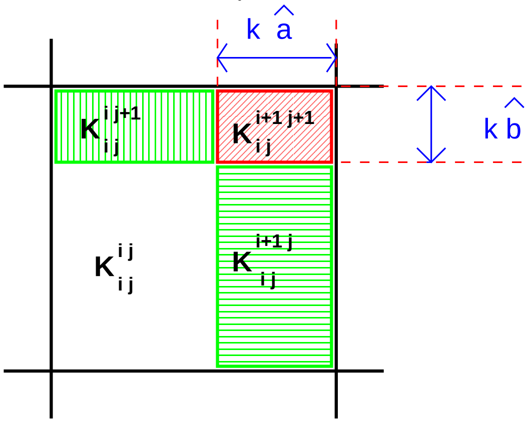

is satisfied. In order to approximate the backwards characteristic flow for one timestep, we shift the vertical interfaces $I_{i,j+\frac{1}{2}}$ horizontally by $(-k\,\widehat{a}^n_{i+\frac{1}{2},j})$ and the horizontal interfaces $J_{i,j+\frac{1}{2}}$ vertically by $(-k\ \widehat{b}^n_{i,j+\frac{1}{2}})$. Depending on the signs of the velocities $\widehat{a}$ and $\widehat{b}$, each cell K_{ij} will be divided into one up to nine sub-rectangles, leading to a natural subdivision

$$K_{ij} = \bigcup_{i',j'} K_{ij}^{i',j'}$$

(compare Figure 2). For example,

$$\begin{aligned}
K_{ij}^{i+1,j} &= K_{ij} \cap ([x_{i+\frac{1}{2}} - k\,\widehat{a}^n_{i+\frac{1}{2},j}, x_{i+\frac{1}{2}}] \times [y_{j-\frac{1}{2}} - k\,\widehat{b}^n_{i,j-\frac{1}{2}}, y_{j+\frac{1}{2}} - k\,\widehat{b}^n_{i,j+\frac{1}{2}}]) \\
K_{ij}^{i+1,j+1} &= K_{ij} \cap ([x_{i+\frac{1}{2}} - k\,\widehat{a}^n_{i+\frac{1}{2},j}, x_{i+\frac{1}{2}}] \times [y_{j+\frac{1}{2}} - k\,\widehat{b}^n_{i,j+\frac{1}{2}}, y_{j+\frac{1}{2}}])
\end{aligned}$$

and so on.

3.3.1. *The MoT-ICE-P0*

In order to define the MoT-ICE-P0, we approximate φ by piecewise constants and define the auxiliary transport velocities by

$$\begin{aligned}
\widehat{a}_{i+\frac{1}{2},j} &= a(x_{i+\frac{1}{2}}, y_j, t_n) + h\,\widetilde{a}_{i+\frac{1}{2},j} &= (a + h\,\widetilde{a})_{i+\frac{1}{2},j} \\
\widehat{b}_{i,j+\frac{1}{2}} &= b(x_i, y_{j+\frac{1}{2}}, t_n) + h\,\widetilde{b}_{i+\frac{1}{2},j} &= (b + h\,\widetilde{b})_{i,j+\frac{1}{2}},
\end{aligned}$$

where the remainders $\widetilde{a}_{i+\frac{1}{2},j}$ and $\widetilde{b}_{i,j+\frac{1}{2}}$ are supposed to be lipschitz-continuous.

Theorem 7 *Suppose that $\lambda = k/h$ is fixed, and that the CFL-condition (8) is satisfied. Then for any given smooth velocity field $\mathbf{a} : \mathbf{R}^2 \times \mathbf{R}_+ \to \mathbf{R}^2$, the MoT-ICE-P0 is consistent of order one with the differential equation (6).*

Note that the theorem states global first order consistency. The difficulty is to control the truncation error near points where the characteristic velocities change sign. See [NOE 99] for the full proof.

3.3.2. *The MoT-ICE-P1*

Let us next construct a scheme based on piecewise linear reconstructions, the MoT-ICE-P1. We have to define the auxiliary transport velocities at the interfaces and the piecewise linear reconstruction of the solution φ.

We denote the piecewise linear reconstruction of φ by φ_R: For $(x,y) \in K_{ij}$ let

$$\varphi_R^{ij}(x,y) := \overline{\varphi}_{ij} + (x - x_i)(\overline{\varphi_x})_{ij} + (y - y_j)(\overline{\varphi_y})_{ij}. \tag{9}$$

A rather involved computation leads to the following choice of auxiliary transport velocities at the interfaces which guarantees second order consistency for smooth solutions:

$$\hat{a}_{i+\frac{1}{2},j} = \left[\left(a + \frac{k}{2}a_t\right)\left(1 - \frac{k}{2}(a_x + b_y)\right) + \frac{k}{2}(ab)_y + k^2\,\widetilde{a}\right]_{i+\frac{1}{2},j} \tag{10}$$

$$\hat{b}_{i,j+\frac{1}{2}} = \left[\left(b + \frac{k}{2}b_t\right)\left(1 - \frac{k}{2}(a_x + b_y)\right) + \frac{k}{2}(ab)_x + k^2\,\widetilde{b}\right]_{i,j+\frac{1}{2}} \tag{11}$$

where $\widetilde{a}$ and $\widetilde{b}$ are supposed to be lipschitz-continuous.

Let us give a geometrical interpretation of these terms: the factors $(a + \frac{k}{2}a_t)$ resp. $(b + \frac{k}{2}b_t)$ simply reflect the fact that we wish to evaluate the transport velocities a resp. b in the center of the space-time interfaces $I_{i+\frac{1}{2},j} \times [t_n, t_{n+1}]$ resp. $J_{i,j+\frac{1}{2}} \times [t_n, t_{n+1}]$ in order to achieve second-order accuracy in time. The factor $(1 - \frac{k}{2}(a_x + b_y))$ which appears both in $\widehat{a}$ and $\widehat{b}$, is an approximation of

$$\exp(-(a_x + b_y)t)$$

at $t = k/2$. This approximates the evolution of φ along the characteristics $\mathbf{z}(\tau; \mathbf{x}, t)$, where (6) gives

$$\frac{d}{d\tau}\varphi(\mathbf{z}(\tau), \tau) = -(\nabla \cdot \mathbf{a}(\mathbf{z}(\tau), \tau))\ \varphi(\mathbf{z}(\tau), \tau).$$

The correction terms $\frac{k}{2}\,(ab)_y$ resp. $\frac{k}{2}\,(ab)_x$ account for fluxes across corners of the grid, see [NOE 99] for a more detailed discussion.

Let us now state the consistency of the MoT-ICE-P1:

Theorem 8 *Let* $\mathbf{a} : \mathbf{R}^2 \times \mathbf{R}_+ \to \mathbf{R}^2$ *be a given smooth velocity field and let* $\varphi : \mathbf{R}^2 \times \mathbf{R}_+ \to \mathbf{R}$ *be a smooth solution of (6).*

Suppose that there are lipschitz-continuous functions $\widetilde{\varphi_x}$ *and* $\widetilde{\varphi_y}$ *such that the piecewise linear reconstruction* φ_R *defined in (9) satisfies*

$$\begin{aligned} (\overline{\varphi_x})_{ij} &= (\varphi_x)_{ij} + h(\widetilde{\varphi_x})_{ij} \\ (\overline{\varphi_y})_{ij} &= (\varphi_y)_{ij} + h(\widetilde{\varphi_y})_{ij} \end{aligned}$$

Let the auxiliary transport velocities $\widehat{a}_{i+\frac{1}{2},j}$ and $\widehat{b}_{i,j+\frac{1}{2}}$ be given by (10) – (11), let $\lambda = k/h$ be fixed and suppose that the CFL-condition (8) holds.

Then the MoT-ICE-P1 is consistent of order two with the differential equation (6).

Once more, we refer to [NOE 99] for the proof, which requires a careful study of the truncation errors of the piecewise linear reconstruction φ_R. Let us stress again that we do obtain second-order consistency at all points, including those where the transport-velocities change sign.

4. Numerical experiments

In this section we present numerical experiments which confirm the accuracy and stability of the new MoT-ICE for smooth and discontinuous solutions.

For the piecewise-linear reconstruction, we choose a central version of the WENO (Weighted Essentially Non-Oscillatory) reconstruction [JS 96]. Details may be found in [NOE 99].

4.1 *Scalar advection with periodic coefficients*

In order to illustrate the failure of consistency of the MoT-CCE-P0 (cell-centered evolution) and the consistency of the new MoT-ICE (interface-centered evolution), we consider the one-dimensional scalar advection equation

$$\partial_t \varphi + \partial_x (\varphi a) = 0$$

over the interval $[-1, 1]$ with

$$a(x, t) \equiv -\sin(\pi x)$$

and

$$\varphi_0(x) \equiv 1.$$

Note that at $x = 0$, $\varphi(0, t)$ satisfies the ordinary differential equation

$$\partial_t \varphi(0, t) = \pi \varphi(0, t),$$

so

$$\varphi(0, t) = e^{\pi t}$$

Similarly,

$$\varphi(1, t) = e^{-\pi t}$$

and these are the maximum and minimum of the exact solution. We compute the solution at time $T = \log(2)/\pi$, so

$$0.5 \leq \varphi(x, T) \leq 2.$$

Table 1: EOCs for one-dimensional advection with periodic coefficients

MoT-CCE-P0				
ix	L_1	EOC	L_∞	EOC
40	5.456309e-02	–	3.439066e-01	–
80	3.210264e-02	0.77	4.215299e-01	-0.29
160	1.731594e-02	0.89	4.617376e-01	-0.13
320	8.996724e-03	0.94	4.813319e-01	-0.06
640	4.587514e-03	0.97	4.908176e-01	-0.03
MoT-ICE-P0				
ix	L_1	EOC	L_∞	EOC
40	3.075886e-02	–	8.834546e-02	–
80	1.599486e-02	0.94	4.741382e-02	0.90
160	8.114853e-03	0.98	2.471667e-02	0.94
320	4.094363e-03	0.99	1.263470e-02	0.97
640	2.055908e-03	0.99	6.379015e-03	0.99
MoT-ICE-P1 with WENO-limiter				
ix	L_1	EOC	L_∞	EOC
40	2.193228e-03	–	5.123679e-03	–
80	5.330401e-04	2.04	1.532804e-03	1.74
160	1.281400e-04	2.06	3.878244e-04	1.98
320	2.993688e-05	2.10	7.604266e-05	2.35
640	5.934229e-06	2.33	1.523297e-05	2.32

We choose a CFL-number of $4\log(2)/\pi$, roughly 0.88. In Table 1, we list the experimental orders of convergence (EOCs) both with respect to the L^1 and L^∞ norm.

In the L^1-norm, the EOC of the MoT-CCE-P0 starts at 0.77 and increases towards 1. However, the method **diverges** in L^∞, as it should have been expected from Example 6 in Section 3.2. Contrary to that, the MoT-ICE converges uniformly (i.e. in L^1 **and** L^∞) to the expected orders. Comparing the L^1 errors of the MoT-CCE-P0 and the MoT-ICE-P0 (piecewise constant reconstructions), one sees that the MoT-ICE converges with a better rate (especially on the coarser grids) and produces roughly half the error of the MoT-CCE. The convergence rates of the MoT-ICE-P1 (piecewise linear reconstructions) are even better than 2 on the finer grids, both for the unlimited and the limited version (we omit the table for the unlimited scheme). The error of the scheme using WENO-limiter is only slightly larger than that of the unlimited scheme and it is of course orders of magnitude smaller than that of the first order MoT-ICE-P0.

4.2 *Rotating Smooth Hump*

Our next test problem is the two-dimensional scalar equation (6) with

$$\begin{aligned} a(x,y,t) &:= -y \\ b(x,y,t) &:= x \end{aligned}$$

in the domain $[-1,1]^2$. Note that on this problem, the MoT-CCE-P0 and the MoT-ICE-P0 will produce identical results, since $a_x \equiv b_y \equiv 0$, so

$$\widehat{a}_{i+\frac{1}{2}j} = a_{i+\frac{1}{2}j} = a_{ij} = -y_j \text{ for all } j$$

and

$$\widehat{b}_{ij+\frac{1}{2}} = b_{ij+\frac{1}{2}} = b_{ij} = x_i \text{ for all } i.$$

We compute one full rotation, i.e. $T = \pi$, and fix $\lambda = \Delta t/\Delta x = \pi/6$. Assuming that the maximal transport velocity is $\sqrt{2}$, this corresponds to a CFL-number of roughly 0.74.

First, we consider smooth initial data. Let $x_0 := 0.5$, $y_0 := 0$, $r_0 := 0.3$,

$$r(x,y) := \left((x-x_0)^2 + (y-y_0)^2\right)^{\frac{1}{2}}$$

Table 2: EOCs for smooth rotating hump.

MoT-ICE-P0					
ix	L_1	EOC	L_∞	EOC	Height
40	9.528519e-01	–	7.129756e-01	–	0.287
80	6.479957e-01	0.56	5.459218e-01	0.39	0.454
160	3.994583e-01	0.70	3.690224e-01	0.56	0.631
320	2.277596e-01	0.81	2.228099e-01	0.73	0.777
640	1.228174e-01	0.89	1.239005e-01	0.85	0.876
MoT-ICE-P1 with unlimited central differences					
ix	L_1	EOC	L_∞	EOC	Height
40	2.596250e-01	–	2.056520e-01	–	0.794
80	5.505040e-02	2.24	4.491245e-02	2.20	0.961
160	1.091899e-02	2.33	8.892373e-03	2.34	0.995
320	2.426323e-03	2.17	1.967944e-03	2.18	0.999
640	5.822946e-04	2.06	4.673955e-04	2.07	1.000
MoT-ICE-P1 with WENO-limiter					
ix	L_1	EOC	L_∞	EOC	Height
40	4.351708e-01	–	4.749751e-01	–	0.525
80	1.201747e-01	1.86	2.327933e-01	1.03	0.767
160	3.337591e-02	1.85	1.018161e-01	1.19	0.898
320	6.350393e-03	2.39	4.022132e-02	1.34	0.960
640	1.030164e-03	2.62	1.230235e-02	1.71	0.988

and

$$\varphi_0(x,y) := \begin{cases} \frac{1}{4}\left(1+\cos(\pi\, r(x,y)/r0)\right)^2 & \text{if } r < r_0, \\ 0 & \text{otherwise.} \end{cases}$$

For the MoT-ICE-P0 the EOCs increase slowly towards unity both in L^1 and L^∞ (see Table 2). The error is very large on the coarser grids, and the convergence is initially slow. This is natural, since the initial data are not well resolved on the coarse grids, where they appear rather as a sharp peak than a smooth hump.

For the MoT-ICE-P1 with unlimited central differences the EOCs are better than two both in L^1 and L^∞ and they converge towards two as the grids are refined. For the MoT-ICE-P1 with WENO-Limiter, the EOCs in L^1 are slightly below two in the beginning. However, as the grid is refined, the EOCs increase drastically and well beyond two. In L^∞, the EOCs start slightly above unity on the underresolved coarse grids, but show a similar dramatic increase as the grids are refined. In our experience, this behavior is typical for the central WENO-limiter.

4.3 *Rotating Cylinder*

Next, we consider the rotating cylinder:

$$\varphi_0(x,y) := \begin{cases} 1 & \text{if } r < r_0, \\ 0 & \text{otherwise.} \end{cases}$$

Since the solution is discontinuous, we only give the experimental orders of convergence in L^1 (see Table 3). We also display the maximal height of the cylinder, in order to see if it is excessively smeared, or whether there are overshoots in the numerical solution. For the MoT-ICE-P0, the EOCs tend towards 0.5 as expected for a linear problem and a scheme based on piecewise constant reconstructions. The maximal height of the cylinder increases towards 1.0 as the grid is refined. For the unlimited MoT-ICE-P1 (we omit the table), the EOCs are decreasing from 0.78 towards 0.70. As should be expected for a

Table 3: EOCs for rotating cylinder.

	MoT-ICE-P0			MoT-ICE-P1, WENO-limiter		
ix	L_1	EOC	Height	L_1	EOC	Height
40	7.012658e-01	–	0.868	3.758964e-01	–	0.993
80	5.046964e-01	0.47	0.968	2.278516e-01	0.72	1.000
160	3.618134e-01	0.48	0.990	1.398394e-01	0.70	1.000
320	2.583896e-01	0.49	0.995	8.588859e-02	0.70	1.000
640	1.837913e-01	0.49	0.997	5.270885e-02	0.70	1.000

Figure 3: Rotating cylinder. MoT-ICE-P0 and MoT-ICE-P1, 160 $\times$ 160 points.

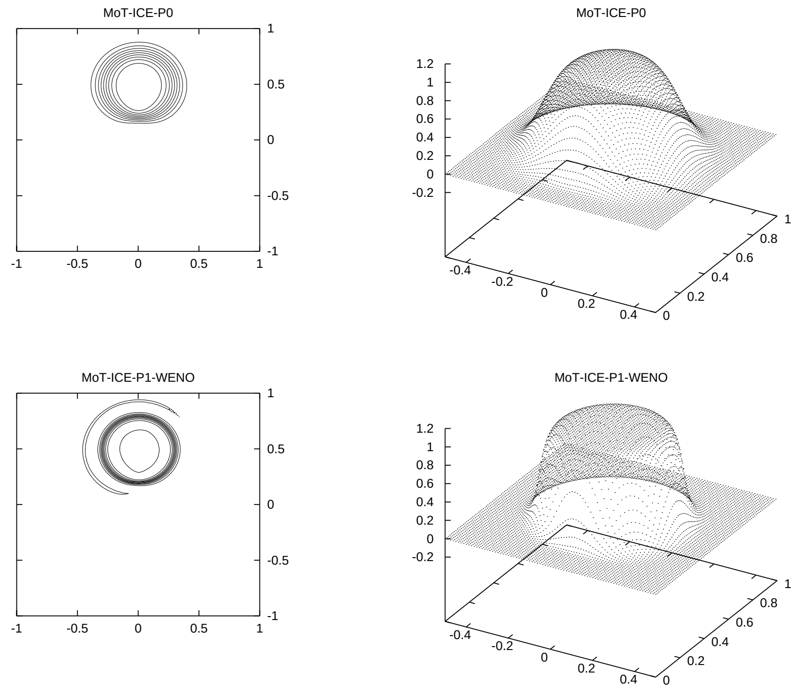

discontinuous solution computed with unlimited piecewise-linear reconstructions, there is an overshoot of 9 to 11 percent of the height of the cylinder. The MoT-ICE-P1 with WENO-limiter converges at rate 0.70, produces no overshoots and only slightly larger L^1-errors than the unlimited scheme. As can be seen from the maximal height especially on the coarser grids, the computation is much less smeared than the one with the MoT-ICE-P0. The error on the finest grid is a factor 3.5 smaller for the limited MoT-ICE-P1 than for the MoT-ICE-P0. Figure 3 shows that the cylindrical shape of the solution is nicely preserved by both versions of the scheme.

4.4 *Shallow-Water-Equations*

In her dissertation [MOR 97], Morel reports glitches at sonic points for a radially symmetric explosion for the shallow-water equations computed with the MoT-CCE-P0. Results using the new MoT-ICE, both P0 and P1, show no such glitches, and produce almost perfectly radially symmetric solutions (see Figure 4). From these pictures, the results of the MoT-ICE-P1 seem to

Figure 4: Explosion problem for the shallow water-equations. MoT-CCE-P0, MoT-ICE-P0, MoT-ICE-P1. Grid of 160 $\times$ 160 Points. Left Column: 25 Contours of water-height. Right Column: cross-sections along the x-axis "+" and the diagonal "$\times$".

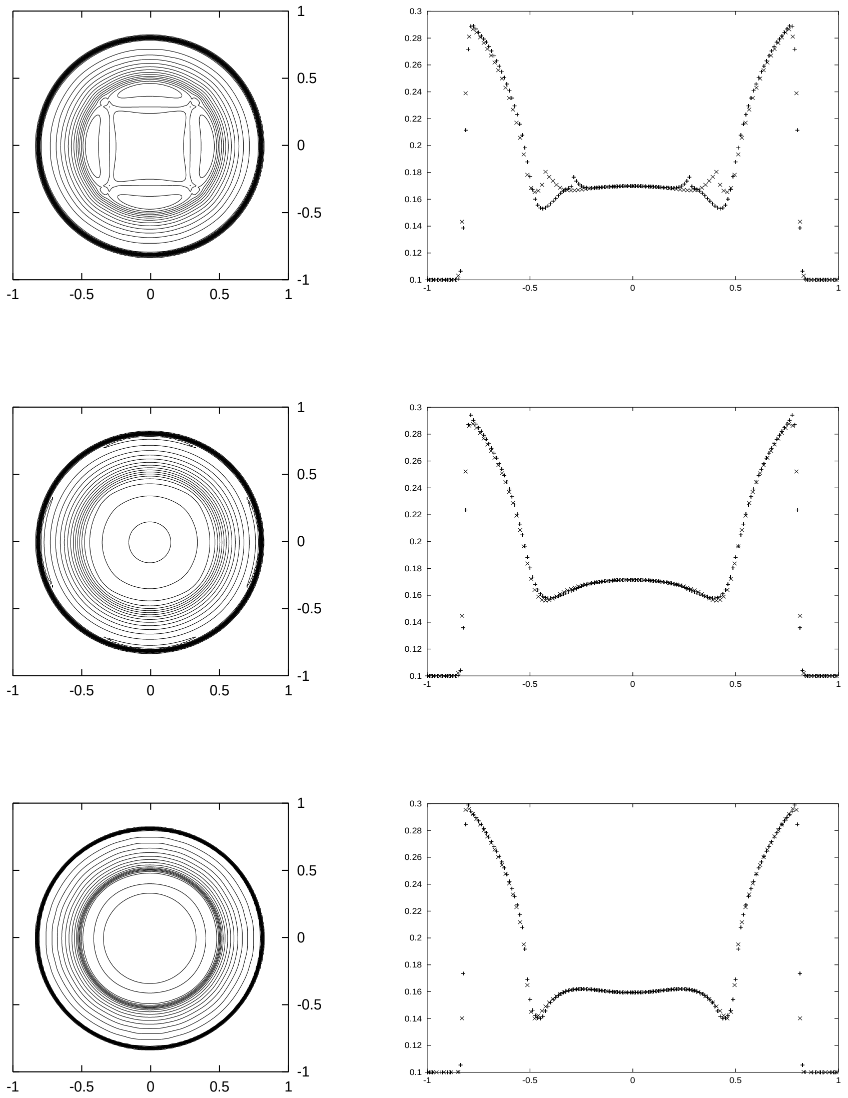

be of the same quality as those computed by Morel using CLAWPACK (see [NOE 99] for crucial implementation-details for the MoT-ICE-P1 for systems of conservation laws).

4.5 *Comparison of efficiencies*

Let us give a first comparison of efficiencies. Morel reports that the MoT-CCE-P0 (which is inconsistent at sonic points), Van Leer's flux-vector-splitting and CLAWPACK $T^{1,0}$ (using the first-order Roe-solver without transverse wave-propagation) all use the same amount of cpu-time (say one time unit). CLAWPACK $T^{1,1}$ takes 1.5 units, and the first-order fix at sonic points proposed by Morel 2.9 units. Our preliminary experience with the MoT-ICE is the following: the MoT-ICE-P0, which is consistent at sonic points, takes 0.9 units and is hence as fast as standard first order schemes. The MoT-ICE-P1 takes 2.2 units, which is the sames as the second order CLAWPACK $T^{2,2}$. This compares favorably with the MoT-CCE-P1, which is consistent at sonic points, but needs 10.5 units of cpu-time.

5. Discussion

The new Method of Transport with Interface-Centered-Evolution (MoT-ICE) is consistent at sonic points, second-order-accurate for smooth solutions and nonoscillatory at discontinuities. In all test-calculations carried out by the author so far it produces high-resolution approximations of multi-dimensional phenomena with almost no grid-orientation effects. It needs about the same CPU-time as a second order version of LeVeque's wave-propagation algorithm CLAWPACK which, according to numbers given by Morel, is 4 to 5 times faster than the original second-order-accurate MoT-CCE-P1. In ongoing joint work with von Törne, we plan to develop the MoT-ICE into a fully adaptive code, capable of handling general geometries.

The multidimensional core of the Method of Transport are Fey's wave-models. Both for theoretical and practical reasons, it would be desirable to establish a systematic approach for their derivation. Are there wave-models for any hyperbolic system of conservation laws, or do they require special symmetries, which are satisfied by the fluid-dynamical equations for which wave-models have been found so far? Which properties should a good wave-model have, besides the formal consistency-requirements (2)-(3)? Can one analyze the interplay between properties of the wave-model and the stability and efficiency of the resulting wave-propagation algorithm?

Let me make one final remark: I would very much like to see a more widespread continuation of the "Great Riemann-Solver Debate" started by Quirk [QUI 94]. Are the failures of Riemann-solver-based schemes reported by Quirk of a cosmetic nature, visible only in the "picture-norm", or can they be quantified? Do the schemes diverge or converge when the grid is refined? How do the so-called "genuinely multi-dimensional" schemes perform in these situations?

6. Bibliography

For lack of space, we do not attempt to give a well-balanced (much less a comprehensive) bibliography. However, the following list should contain lots of useful information:

[BT 97] Billet, S. and Toro, E., *On WAF-type schemes for multidimensional hyperbolic conservation laws.* J. Comput. Phys. 130 (1997), 1 – 24.

[CCL 94] Cockburn, B., Coquel, F. and LeFloch, P., *Convergence of the finite volume method for multidimensional conservation laws.* SIAM J. Numer. Anal. 32 (1995), 687 – 705.

[COL 90] Colella, P., *Multidimensional upwind methods for hyperbolic conservation laws.* J. Comput. Phys. 87 (1990), 171 – 200.

[FEY 98a] Fey, M. *Multidimensional upwinding. I. The method of transport for solving the Euler equations.* J. Comput. Phys. 143 (1998), 159 – 180.

[FEY 98b] Fey, M. *Multidimensional upwinding. II. Decomposition of the Euler equations into advection equations.* J. Comput. Phys. 143 (1998), 181 – 199.

[FJMM 97] Fey, M., Jeltsch, R., Maurer, J. and Morel, A.-T., *The method of transport for nonlinear systems of hyperbolic conservation laws in several space dimensions.* Research Report No.97-12, Seminar for Applied Mathematics, ETH Zürich (1997).

[HIR 90] Hirsch, C., *Numerical computation of internal and external flows.* Vol.2, Wiley-Interscience 1990.

[JS 96] Jiang, G.-S. and Shu, C.-W., *Efficient implementation of weighted ENO schemes.* J. Comput. Phys. 126 (1996), 202 – 228.

[KNR 95] Kröner, D., Noelle, S. and Rokyta, M., *Convergence of higher order upwind finite volume schemes on unstructured grids for scalar conservation laws in several space dimensions.* Numer. Math. 71 (1995), 527 – 560.

[LEV 97] LeVeque, R.J., *Wave Propagation Algorithms for Multidimensional Hyperbolic Systems.* J. Comput. Phys. 131 (1997), 327 – 353.

[LW 92] LeVeque, R.J. and Walder, R., *Grid alignment effects and rotated methods for computing complex flows in astrophysics.* eds. J.B. Vos, A. Rizzi and I.L. Rhyming, Proceedings of the Ninth GAMM Conference on numerical methods in fluid mechanics. Notes Num. Fluid. Mech. 35 (1992), 376–385.

[LMW 97] Lukacova-Medvidova, M., Morton, K. and Warnecke, G. *Evolution Galerkin methods for hyperbolic systems in two space dimensions.* Report 97-44, Univ. Magdeburg, Germany (1997).

[MOR 97] Morel, A.-T., *A genuinely multidimensional high-resolution scheme for the shallow-water equations.* Dissertation, ETH Zürich Diss. No. 11959 (1997).

[NOE 94] Noelle, S., *Hyperbolic systems of conservation laws, the Weyl equation, and multi-dimensional upwinding.* J. Comput. Phys. 115 (1994), 22 – 26.

[NOE 96] Noelle, S., *A note on entropy inequalities and error estimates for higher order accurate finite volume schemes on irregular families of grids.* Math. Comp. 65 (1996), 1155 –1163.

[NOE 99] Noelle, S., *The MoT-ICE: a new high-resolution wave-propagation algorithm for multi-dimensional hyperbolic systems of conservation laws based on Fey's Method of Transport.* To be submitted for publication, 1999.

[QUI 94] Quirk, J., *A Contribution to the Great Riemann Solver Debate.* Int. J. Numer. Meth. Fluid Dyn. 18 (1994), 555 – 574.

[ROE 86] Roe, P., *Discrete models for the numerical analysis of time-dependent multidimensional gas dynamics.* J. Comput. Phys. 63 (1986), 458 – 476.

[ROE 91] Roe, P., *Discontinuous solutions to hyperbolic systems under operator splitting.* Numer. Meth. Part. Diff. Eq. 7 (1991), 207.

[SW 81] Steger, J. and Warming, R., *Flux vector splitting of the inviscid gas-dynamic equations with applications to finite difference methods.* J. Comput. Phys. 40 (1981), 263 – 293.

[VNL 92] Van Leer, B., *Progress in multi-dimensional upwinding.* ICASE Report 92-43 (1992).

[WN 99] Westdickenberg, M. and Noelle, S., *A new convergence proof for finite volume schemes using the kinetic formulation of conservation laws.* Accepted for publication in SIAM J. Numer. Anal. (Feb. 1999).